Available online at www.sciencedirect.com

ScienceDirect

Mendeleev Commun., 2017, **27**, 583–585

Mendeleev Communications

Codeposition of platinum and palladium onto molybdenum bronzes under open-circuit conditions and the electrooxidation of methanol on the resulting catalysts

Roman S. Batalov,[a] Vitaly V. Kuznetsov,*[a] Boris I. Podlovchenko[b] and Vadim A. Zaytsev[a]

[a] *Department of General and Inorganic Chemistry, D. I. Mendeleev University of Chemical Technology of Russia, 125047 Moscow, Russian Federation. Fax: +7 499 978 9484; e-mail: vitkuzn1@mail.ru*

[b] *Department of Chemistry, M. V. Lomonosov Moscow State University, 119991 Moscow, Russian Federation. Fax: +7 495 939 0171; e-mail: podlov@elch.chem.msu.ru*

DOI: 10.1016/j.mencom.2017.11.015

The composites nPt·mPd·($H_{x-2(n+m)}MoO_3$) showed a much higher activity in methanol oxidation in comparison with electrodeposited platinum.

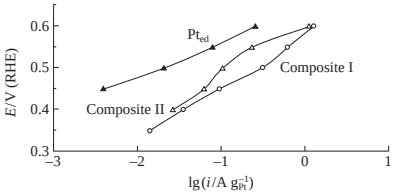

Recently, attention has been focused on the use of electrode materials containing platinum and the oxo compounds of molybdenum, *e.g.*, molybdenum bronzes, as anodes for hydrogen-oxygen and direct methanol fuel cells.[1–4] The promoting effect of molybdenum compounds on the methanol electrooxidation reaction (MOR) is associated with the acceleration of the oxidation of chemisorbed species (mainly CO_{ads}), which block the oxidation of MeOH through tight bonding with the electrode surface adsorbed particles.[4–10] Platinum deposition onto the surface of hydrogen-containing molybdenum bronzes under open-circuit conditions is promising for enhancing the specific activity of Pt.[4] The nPd·($H_{x-2n}MoO_3$) catalyst, whose activity is not inferior to that of Pt, was synthesized.[9,10] A synergistic catalytic effect toward the MOR on mixed Pt–Pd catalysts was found.[11–13] The partial replacement of platinum by less expensive and less scarce palladium is of practical interest. The aim of this study was (i) to prepare mixed Pt–Pd–H_xMoO_3 catalysts by deposition onto hydrogen-containing molybdenum bronzes under open-circuit conditions and (ii) to measure their catalytic activity.

The reactions occurring on the currentless deposition of platinum and palladium onto molybdenum bronze† can be represented by the overall equation (1).

$$n\mathrm{PtCl_4^{2-}} + m\mathrm{Pd^{2+}} + \mathrm{H_xMoO_3} \rightarrow \rightarrow n\mathrm{Pt}\cdot m\mathrm{Pd}\cdot(\mathrm{H_{x-2(n+m)}MoO_3}) + 2(n+m)\,\mathrm{H^+} + 4n\,\mathrm{Cl^-} \quad (1)$$

Although this reaction seems to be the dehydrogenation of molybdenum bronze, the Mo oxidation state actually increased.[9,10] Note that n and m are not integers.

The rapid increase of the electrode potential up to ~0.26 V [Figure 1(*b*)] is observed after bringing red molybdenum bronze into contact with a solution containing K_2PtCl_4 and $PdCl_2$ in small concentrations (Table 1, Solution I). According to the anodic scan of CVAs of H_xMoO_3 [Figure 1(*a*)], this potential corresponds to the red-ox transitions of molybdenum bronze. After that, the prolonged plateau was observed in the *E vs. t* curve. The conjugate reactions of molybdenum bronze oxidation and Pt and Pd deposition occur under these conditions at the electrode surface. The chemical analysis data revealed that the ratio of Pt and Pd atomic fractions in the deposit p(Pt)/p(Pd) = p and the solution greatly differed even when the concentration of the salts was below 10^{-3} M. Consequently, the red-ox reactions were not diffusion controlled.

As follows from the results of chemical analysis (Table 1), the value of p for the composite obtained from Solution I is 7.6; this

† The reagents used in the experiments were described elsewhere.[4,9,10] The red molybdenum bronze was uniformly spreaded onto the surface of a glassy carbon (GC) electrode (S_{geom} = 1 cm^2) without a binder. The weight of molybdenum bronze was 2±0.2 mg, and the average thickness of the molybdenum bronze layer was 5 μm. The electrode with molybdenum bronze was placed in a 0.5 M deaerated aqueous solution of H_2SO_4. The electrode was polarized at a potential of 0 V [electrode potentials are given *vs.* a reversible hydrogen electrode (RHE) in the same solution] during 30 min for the additional reduction of molybdenum bronze. After that, the external polarization was switched off, and the solution of sulfuric acid was replaced by the solution containing K_2PtCl_4 and $PdCl_2$ in 0.5 M H_2SO_4. The potential–time transient (*E vs. t*) was fixed in the course of Pt and Pd deposition under open-circuit conditions. The weights of the deposited Pt and Pd were determined by the dissolution of nPt·mPd·($H_{x-2(n+m)}MoO_3$) in *aqua regia* followed by the analysis of the solution using inductively coupled plasma atomic emission spectrometry (AES ICP). The morphology of prepared composites was studied by scanning electron microscopy (SEM). The images of the electrode surfaces were obtained on a Hitachi TM-3000 electron microscope with an X-ray microanalyzer. The chemical composition of the surface layers was studied by X-ray photoelectron spectroscopy (XPS) using an HB100 spectrometer (Vacuum Generators) with AlKα radiation ($h\nu$ = 1486.6 eV, 200 W).

All electrochemical measurements were performed in a standard three-electrode electrochemical cell in an argon atmosphere. An IPC-Pro digital potentiostat was used. The electrochemically active surface area (EASA) was determined by measuring the charge corresponding to the CO_{ads} monolayer desorption as described previously.[4,10] The electrooxidation of methanol was carried out under potentiostatic conditions at E = 0.35–0.60 V in a solution containing 1.0 M MeOH and 0.5 M H_2SO_4. The stationary currents of methanol oxidation were measured, and the stationarity criterion was set to a current change of less than 1% per minute.

Table 1 Solutions for the currentless deposition of Pt and Pd onto molybdenum bronzes and some properties of the deposits.

Solution	Concentration / mmol dm^{-3}		$c(Pt^{II})/c(Pd^{II})$, in the solution	t_{dep}/s	Weight of deposited metal / μg		p(Pt)/p(Pd), in the bulk of deposit	S_{Pt+Pd}/cm^2	p(Pt)/p(Pd), at the surface of deposit
	K_2PtCl_4	$PdCl_2$			Pt	Pd			
I	0.8	0.15	5.30	16000	28	2	7.60	3.1	7.20
II	7.0	14.00	0.50	1000	106	182	0.32	20.6	0.25

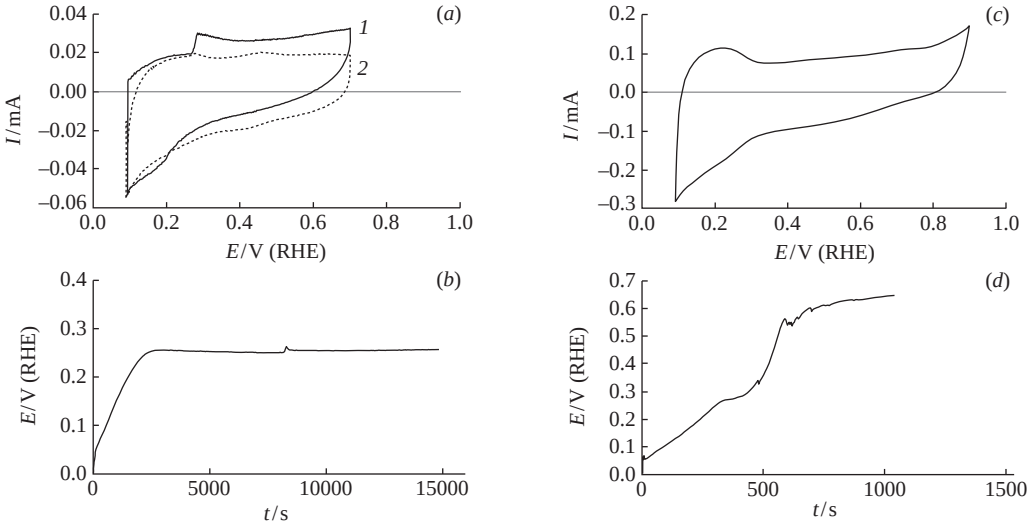

Figure 1 (*a*) Cyclic voltammograms (v = 2 mV s^{-1}) of (*1*) H_xMoO_3/GC, (*2*) nPt·mPd·($H_{x-2(n+m)}MoO_3$)/GC (p = 7.6) in 0.5 M H_2SO_4; (*b*) *E vs. t* during the preparation of Composite I; (*c*) cyclic voltammogram (v = 2 mV s^{-1}) of nPt·mPd·($H_{x-2(n+m)}MoO_3$)/GC (p = 0.32) in 0.5 M H_2SO_4 and (*d*) *E vs. t* during the preparation of Composite II.

material contains platinum doped by a small amount of palladium. This electrode is referred to as nPt·mPd·($H_{x-2(n+m)}MoO_3$)/GC (p = 7.6) or Composite I. Using the weights of deposited Pt and Pd, we can calculate that $n + m$ = 0.03, as described previously;[4] *i.e.*, only a small increase in the oxidation state of Mo atoms occurred under the conditions of currentless deposition of Pt and Pd from solution containing low concentrations of their salts.

The concentrations of platinum and palladium salts were increased by a factor of about 10 to obtain more massive metal deposits (Table 1, Solution II). In this case, the rate of reaction became much higher, and the duration of potential delay at E = 0.26 V on *E vs. t* curves was greatly reduced [Figure 1(*d*)]. The growth of electrode potential up to 0.7 V was further observed, and this fact is consistent with published data.[9,10] The electrode with p = 0.32, *i.e.*, with an increased Pd content, was obtained from Solution II. It was referred to as nPt·mPd·($H_{x-2(n+m)}MoO_3$)/GC (p = 0.32) or Composite II. The value of $n + m$ was ~0.35, *i.e.* deeper oxidation of molybdenum bronze in comparison with Solution I took place.

The deposition of Pt and Pd onto the surface of hydrogen-containing molybdenum bronze leads to the suppression of peaks at potentials of 0.25−0.30 V, which correspond to the red-ox transition of Mo on CVs [Figure 1(*a*),(*c*)]. The asymmetry of cathodic and anodic branches of cyclic voltammograms of nPt·mPd·($H_{x-2(n+m)}MoO_3$) electrodes was observed in the 'hydrogen' region of electrode potentials (0.09–0.30 V). The charge passing through the electrode during the anodic scan of CVs was much smaller than a charge passed during the cathodic scan. This was especially pronounced for the electrode containing a large amount of palladium (Composite II). Apparently, the H_{ads} spillover into the bulk of composite occurred during the measurements, and this led to the asymmetry of CVs. This effect together with possible hydrogen dissolution in the Pt–Pd deposits make incorrect the calculation of EASA based on the charge measured in the 'hydrogen' region of potentials.

The SEM investigations revealed that the distributions of Pt and Pd over the surfaces of Composites I and II were noticeably different [Figure 2(*a*),(*c*)]. More often, platinum and palladium were codeposited onto the surface of molybdenum bronze particles. However, the separated Pd clusters were fixed at the surface of Composite I [yellow spots in Figure 2(*b*)]. A rather uniform deposition of Pt–Pd alloy was observed in the case of Composite II. The XPS data showed that the ratios of Pt and Pd atomic fractions at the electrode surface and in the volume of composites differed slightly (see Table 1). At the first sight, this fact contradicts the formation of not only Pt–Pd but also Pd clusters. However, XPS gives only an average magnitude; the spot diameter was approximately 600 μm.

The electrochemical desorption of CO_{ads} from the surface of platinum metals allows us to estimate the electrocatalytic properties of electrode materials for the oxidation reactions of small organic

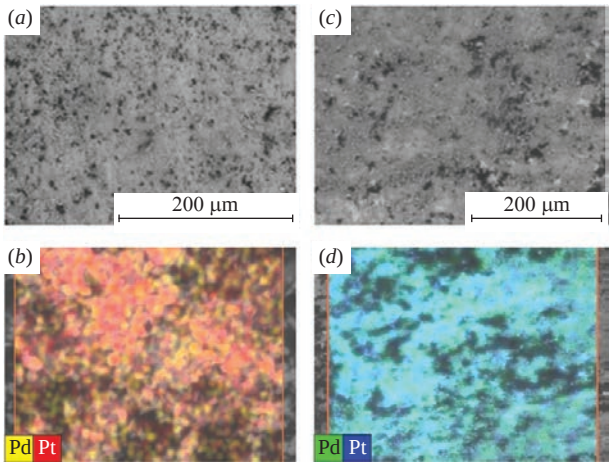

Figure 2 SEM images of Composites (*a*) I and (*b*) II and the distribution of Pt and Pd over surface of Composites (*c*) I and (*d*) II.

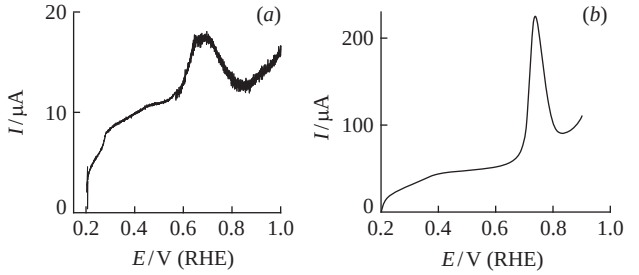

Figure 3 The electrodesorption of a CO_{ads} monolayer from the surfaces of (*a*) *n*Pt·*m*Pd·($H_{x-2(n+m)}MoO_3$)/GC (*p* = 7.6) and (*b*) *n*Pt·*m*Pd·($H_{x-2(n+m)}MoO_3$)/GC (*p* = 0.32) electrodes in 0.5 M H_2SO_4. *v* = 1 mV s^{-1}.

molecules since the strongly bonded species, which block the active centers at the electrode surface, are mostly CO_{ads}.[14–16] The results of detailed studies on strongly bonded chemisorbed species containing carbon revealed[17,18] that their composition was much more complicated. In addition to CO_{ads}, HCO_{ads} and other species were present at the electrode surface.[17,18] Despite this fact, the regularities of CO_{ads} electrodesoption often correlated with the catalytic activity of electrodes.[19]

A broad peak of CO_{ads} electrodesorption with a maximum at ~0.7 V [Figure 3(*a*)] was observed in the potentiodynamic polarization curve for *n*Pt·*m*Pd·($H_{x-2(n+m)}MoO_3$)/GC (*p* = 7.6). A similar peak with E_{max} = 0.68 V was obtained for *n*Pt·($H_{x-2n}MoO_3$).[4] Thus, we can assume that the catalytic activity of these two electrodes is comparable. For *n*Pt·*m*Pd·($H_{x-2(n+m)}MoO_3$)/GC (*p* = 0.32), the of CO_{ads} desorption peak maximum was observed at ~0.72 V [Figure 3(*b*)]. This value is much less positive in comparison with that of electrodeposited palladium (Pd_{ed})[20] and does not differ greatly from E_{max} for Composite I.

The specific rates of MOR per square cantimetre of EASA for *n*Pt·*m*Pd·($H_{x-2(n+m)}MoO_3$)/GC (*p* = 7.6) [Figure 4(*a*), curve *1*] were not lower than those for *n*Pt·($H_{x-2n}MoO_3$). According to Figure 4(*a*), we can assume that the activity of platinum deposits doped with the microquantities of Pd (Composite I) was even higher at *E* < 0.55 V. However, this relatively small difference can be related to the incorrect estimation of EASA based on the desorption of CO monolayer, namely, to the inaccuracy of the graphical separation of CO_{ads} oxidation currents from the currents of Mo bronze oxidation (Figure 3) and to the possibility of the adsorption of CO molecules in both a linear and a bridged form. Note that, based on the charge corresponding to the CO monolayer desorption, it is possible to find only the total surface area occupied by both Pt and Pd atoms.[21,22] This makes impossible the separate determination of partial currents of MOR on Pt and Pd.

The specific currents of MOR on Composite I (curve *1*) are significantly higher than those on Pt_{ed}/GC (curve *4*) and especially on Pd_{ed}/GC (curve *5*). For Composite II, the MOR currents [Figure 4(*a*), curve *2*] were somewhat lower in comparison with Composite I, but they were also significantly higher than those

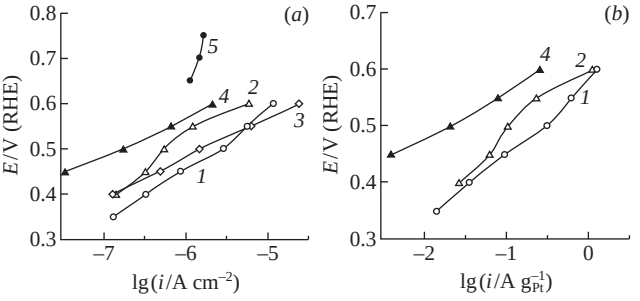

Figure 4 Stationary polarization curves of MOR in a solution containing 1 M MeOH + 0.5 M H_2SO_4 normalized on (*a*) EASA and (*b*) mass of platinum: (*1*) *n*Pt·*m*Pd·($H_{x-2(n+m)}MoO_3$)/GC (*p* = 7.6), (*2*) *n*Pt·*m*Pd·($H_{x-2(n+m)}MoO_3$)/GC (*p* = 0.32), (*3*) *n*Pt·($H_{x-2n}MoO_3$)/GC, (*4*) Pt_{ed}, and (*5*) Pd_{ed}.

on Pt_{ed}/GC (especially at *E* < 0.5 V). Previously,[9,10] we found the high activity of a Pd deposit on the Mo bronze. In this regard, one might expect a not lower activity of Composite II as compared with that of Composite I. However, it was marked[9,10] that the promoting effect of molybdenum oxides toward MOR largely depended on the length of Pd/MoO_x interphase borders, and it was shown[13,21,22] that the activity of mixed Pt–Pd deposits depended on the distribution of Pt and Pd over the electrode surface. The large quantities of palladium in Composite II led to an increase in the portion of Pd atoms, which did not contact with molybdenum bronzes, but the monocomponent Pd catalysts are known to be inactive in MOR. The specific currents of MOR on a platinum weight basis are of great interest for the practice since they show the utilization degree of Pt. Figure 4(*b*) indicates that the mass activity of the mixed deposits with both *p* = 7.6 and 0.32 (curves *1* and *2*) are far superior to the activity of Pt_{ed}/GC. At *E* < 0.55 V, the currents on Composites I and II exceed those on Pt_{ed}/GC by a factor of 5–10 or higher.

This work was supported by the Ministry of Education and Science of the Russian Federation (project no. 4.4584.2017/BY) and the Russian Foundation for Basic Research (project no. 15-03-03436a).

References

1 O. Guillén-Villafuerte, G. García, J. L. Rodríguez, E. Pastor, R. Guil-López, E. Nieto and J. L. G. Fierro, *Int. J. Hydrogen Energy*, 2013, **38**, 7811.
2 H. Wang, X. Wang, J. Zheng, F. Peng and H. Yu, *Chin. J. Catal.*, 2014, **35**, 1687.
3 Y. Hao, X. Wang, Y. Zheng, J. Shen, J. Yuan, A. Wang, L. Niu and S. Huang, *Electrochim. Acta*, 2016, **198**, 127.
4 V. V. Kuznetsov, B. I. Podlovchenko, R. I. Shakurov, K. V. Kavyrshina and S. E. Lyashenko, *Int. J. Hydrogen Energy*, 2014, **39**, 829.
5 P. Justin and G. R. Rao, *Int. J. Hydrogen Energy*, 2011, **36**, 5875.
6 M. V. Martínez-Huerta, J. L. Rodríguez, N. Tsiouvaras, M.A. Peña, J. L. G. Fierro and E. Pastor, *Chem. Mater*., 2008, **20**, 4249.
7 M. Neurock, M. Janik and A. Wieskowski, *Faraday Discuss*., 2008, **140**, 363.
8 E. A. Batista, G. R. P. Malpass, A. J. Motheo and T. Iwasita, *J. Electroanal. Chem*., 2004, **571**, 273.
9 V. V. Kuznetsov, R. S. Batalov and B. I. Podlovchenko, *Russ. J. Electrochem*., 2016, **52**, 408 (*Elektrokhimiya*, 2016, **52**, 463).
10 B. I. Podlovchenko, V. V. Kuznetsov and R. S. Batalov, *J. Solid State Electrochem*., 2016, **20**, 589.
11 X. Yan, T. Liu, J. Jin, S. Devaramani, D. Qin and X. Lu, *J. Electroanal. Chem*., 2016, **770**, 33.
12 F. Alcaide, G. Álvarez, P. L. Cabot, H.-J. Grande, O. Miguel and A. Querejeta, *Int. J. Hydrogen Energy*, 2011, **36**, 4432.
13 T. D. Gladysheva, B. I. Podlovchenko, D. S. Volkov and A. Yu. Filatov, *Mendeleev Commun*., 2016, **26**, 298.
14 R. S. Amin, K. M. El-Khatib, S. Siracusano, V. Baglio, A. Stassi and A. S. Arico, *Int. J. Hydrogen Energy*, 2014, **39**, 9782.
15 A. Hamnett, in *Comprehensive Chemical Kinetics*, eds. R. G. Compton and G. Hancock, Elsevier, Amsterdam, 1999, vol. 37, pp. 635–682.
16 K. Kinumatsu, *Ber. Bunsen-Ges. Phys. Chem*., 1990, **94**, 1025.
17 T. Yajima, H. Uchida and M. Watanabe, *J. Phys. Chem. B*, 2004, **108**, 2654.
18 V. P. Santos, V. Del Colle, R. Batista de Lima and G. Tremiliosi-Filho, *Langmuir*, 2004, **20**, 11064.
19 B. Beden, C. Lamy, N. R. de Tacconi and A. J. Arvia, *Electrochim. Acta*, 1990, **35**, 691.
20 Yu. M. Maksimov and B. I. Podlovchenko, *Russ. J. Electrochem*., 2006, **42**, 408 (*Elektrokhimiya*, 2006, **42**, 461).
21 T. D. Gladysheva, A. Yu. Filatov and B. I. Podlovchenko, *Mendeleev Commun*., 2015, **25**, 56.
22 B. I. Podlovchenko, T. D. Gladysheva and A. Yu. Filatov, *Mendeleev Commun*., 2015, **25**, 293.

Received: 15th March 2017; Com. 17/5202